NASA
Technical Memorandum 105655

AVSCOM
Technical Report 91–C–036

Application of Face-Gear Drives in Helicopter Transmissions

F.L. Litvin and J.-C. Wang
University of Illinois at Chicago
Chicago, Illinois

R.B. Bossler, Jr.
Lucas Western, Incorporated
City of Industry, California

Y.-J.D. Chen and G. Heath
McDonnell Douglas Helicopter Company
Mesa, Arizona

and

D.G. Lewicki
Propulsion Directorate
U.S. Army Aviation Systems Command
Lewis Research Center
Cleveland, Ohio

Prepared for the
Sixth International Power Transmission and Gearing Conference
sponsored by the American Society of Mechanical Engineers
Scottsdale, Arizona, September 13–16, 1992

NASA

US ARMY
AVIATION
SYSTEMS COMMAND

APPLICATION OF FACE-GEAR DRIVES IN HELICOPTER TRANSMISSIONS

F.L. Litvin and J.-C. Wang
University of Illinois at Chicago
Chicago, Illinois 60680

R.B. Bossler, Jr.
Lucas Western, Incorporated
City of Industry, Claifornia 91749

Y.-J.D. Chen and G. Heath
McDonnell Douglas Helicopter Company
Mesa, Arizona 85205

D.G. Lewicki
U.S. Army Propulsion Directorate
Lewis Research Center
Cleveland, Ohio 44135

E-7019

ABSTRACT

The use of face gears in helicopter transmissions was explored. A light-weight, split torque transmission design utilizing face gears was described. Face-gear design and geometry were investigated. Topics included tooth generation, limiting inner and outer radii, tooth contact analysis, contact ratio, gear eccentricity, and structural stiffness. Design charts were developed to determine minimum and maximum face-gear inner and outer radii. Analytical study of transmission error showed face-gear drives were relatively insensitive to gear misalignment, but tooth contact was affected by misalignment. A method of localizing bearing contact to compensate for misalignment was explored. The proper choice of shaft support stiffness enabled good load sharing in the split torque transmission design. Face-gear experimental studies were also included and the feasibility of face gears in high-speed, high-load applications such as helicopter transmissions was demonstrated.

INTRODUCTION

The Advanced Rotorcraft Transmission (ART) program is an Army funded, joint Army/NASA program to develop and demonstrate lightweight, quiet, durable drivetrain systems for next generation rotorcraft (Bill, 1990). One contract team participant, McDonnell Douglas Helicopter Company (MDHC)/Lucas Western Incorporated, developed a novel split torque ART configuration using face gears (Bossler and Heath, 1990, 1991). The geometry and design of face gears and computerized simulation of their meshing have been developed by another member of the team, the University of Illinois at Chicago.

Manufacturing of face gears was proposed many years ago by the Fellows Corporation. Face gears have had widespread use in low power applications but have not had much development of design and manufacturing practice for high power use.

The theory of face-gear drives has not been developed sufficiently for the needs of the designers and manufacturers. Publications in this area in English by E. Buckingham (1949), and D.W. Dudley (1962) can be considered only as a brief description of face-gear drives. J. Davidov (1950), and F.L. Litvin and L.J. LiBurkin (1968) have published the results of their investigation of face-gear drives in Russian literature, but these works are not familiar in the western world.

The advantages of face-gear drives are: (1) reduced sensitivity of the bearing contact to gear misalignment, (2) reduced level of noise due to the very low level of transmission errors, and (3) more favorable conditions of transfer of load from one pair of teeth to the next pair of teeth. Statement (3) is based on the advantage of involute gearing to have a common normal for those teeth that are finishing and starting the meshing.

This paper shows that with proper design face-gear drives can find a successful application in high power applications. The performed research enables provision of sufficient tooth length and localized bearing contact. The results of computerized simulation of meshing and bearing contact and experimental test of face-gear drives confirm that such drives can be successfully applied in power transmissions.

The paper covers application of face-gear drives in helicopter transmission. The advantage of this application is the possibility to split the torque between two face-gear drives. The design of face-gear drives, simulation of meshing and bearing contact, have been computerized and supported by computer programs and design charts. The split of torque has been confirmed by finite element structural analysis. A set of face-gear drives has been successfully tested at NASA Lewis Research Center.

SPLIT TORQUE DESIGN

The idea of the split of torque is illustrated with Fig. 1. Figure 1(a) shows the alternative version of the torque split by two spiral bevel pinions, *a* and *b*, designed as one rigid body. Figure 1(b) shows the second version of the split of torque when a single spur (or helical) pinion is in mesh with two face gears. The advantage of the second version is that the transmitting forces transmit a reduced load on the bearings in comparison with the version shown in Fig. 1(a). A second advantage is that the pinion is a conventional spur (or helical) gear compared to a complex spiral bevel design with two pinions.

The general configuration of the MDHC/Lucas ART design is illustrated conceptually in Fig. 2, although there have been some changes in details since this drawing was made. There are two

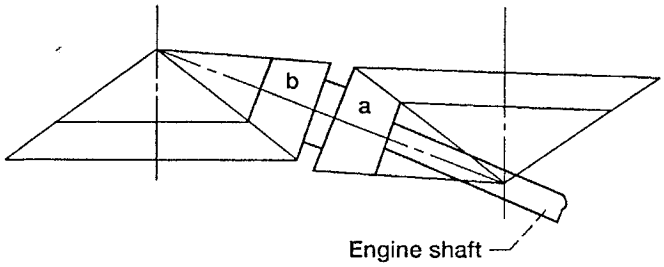

(a) Bevel gear arrangement.

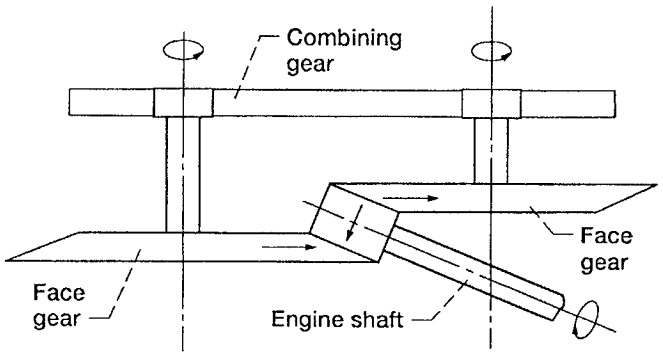

(b) Face-gear arrangement.

Figure 1.—Split-torque configurations.

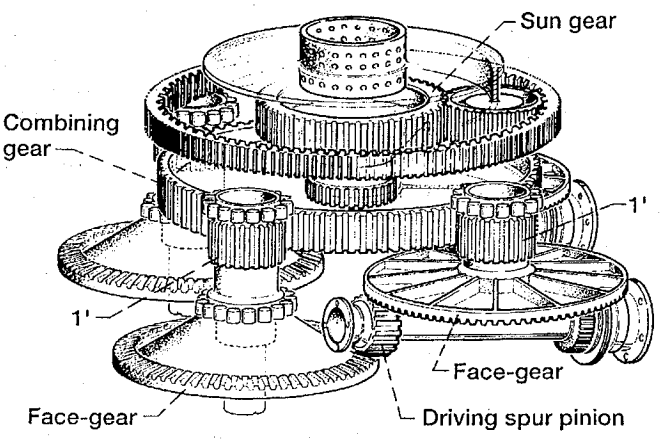

Figure 2.—3-stage split-torque single planetary transmission.

engines rated at 1864 kW (2500 hp) each which combine to drive the rotor shaft with 3728 kW (5000 hp). The transmission is designed to carry 2237 kW (3000 hp) per side for a one engine inoperative condition. Power flows from the engine through an overrunning positive-engagement clutch to a spur pinion, which is radially lightly restrained. The spur pinion drives a downward-facing face gear and an upward-facing face gear. The face-gear shafts terminate in spur pinions, which drive a large combining gear. The hub of the combining gear is attached to the sun gear of a high-contact-ratio planetary gear set where the carrier is the output member and is attached to the rotor shaft. A small pinion is driven at the aft side of the main combining gear. This pinion drives another face gear mounted on the NOTAR™ (no tailrotor) driveshaft, which leads aft directly to a NOTAR™ fan.

The concept of torque split appears to be a significant development wherein an input spur-gear pinion drives two face gears arranged to provide an accurate division of power. This division greatly reduces the size and weight of the corner-turning hardware as well as the size and weight of the next reduction stage. The predicted payoff is greatly reduced weight and cost compared to conventional design.

The pinion which serves the two face gears is a conventional spur gear with an even number of teeth. If the spur gears were rigidly located between the two face gears, precise torque splitting would be very unlikely. The spur gear has a free-floating mount which allows self-centering between the two face gears. It will be shown analytically (see next section) that precise torque splitting (with ±1.0%) will take place.

More importantly, torque splitting between two driven gears by a free-floating spur-gear pinion has been used for many years in truck transmissions. The first known truck application was the experimental Road Ranger transmission produced by the Fuller Transmission Division of the Eaton Manufacturing Company in 1961. Truck transmissions using this principle have been in production since 1963. In addition to accurate torque splitting, it was found that gear noise was reduced and gear life was increased. Thus the use of a free floating pinion as a torque-splitting device is well substantiated.

FINITE ELEMENT STRUCTURAL ANALYSIS FOR THE SPLIT TORQUE GEAR DRIVE

The success of a split-torque gear train design depends on the equal division of the torque to the two output shafts. Conceptually, the floating pinion design makes the system of the pinion shaft a two-force member. The transmitted forces on the two diametrically opposite meshing points on the pinion have to balance each other to achieve equal torque splitting.

The analytical effort to validate the split torque concept was conducted with the use of a finite element method. To analyze the deflection and the percentage of torque splitting in real condition, the elasticity of the gear structure and the shaft has to be considered first. The finite element model provides an accurate approach to include the stiffness and the deflection of the gear structure. The overall model of the split-torque gear train is shown in Fig. 3. The

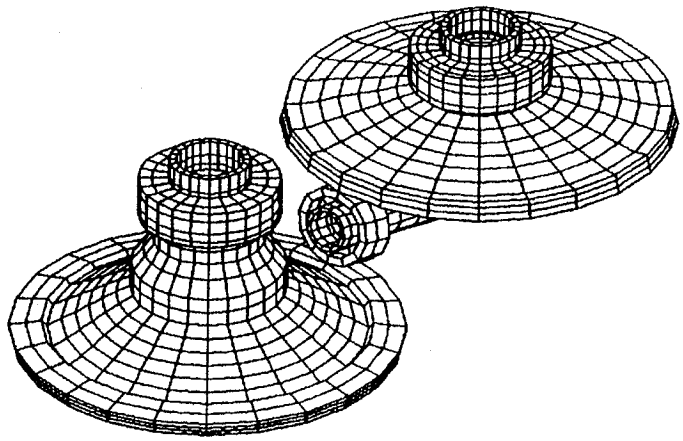

Figure 3.—Finite element model of the split-torque drive.

model has been used to analyze the torque splitting percentage for different support conditions as shown in Table I. The stiffnesses of the front and rear support of the pinion shaft were varied to determine their effect on torque split (cases 1 to 4, Table I). The contacts between the pinion and the two face gears were modeled using gap elements. The torque split was determined using gap element reaction forces as calculated using finite element analysis. Among the first four cases studied, the most even torque split was provided in case 4 when the stiffness of the shaft's front support was 1.1×10^7 N/m (6.0×10^4 lb/in.). This is an order of magnitude less than a typical bearing support and is realistic.

TABLE I. — ADVANCED ROTORCRAFT TRANSMISSION TORQUE SPLITTING PERCENTAGES

Case number	Support of pinion shaft		Gear meshing clearance, mm (in.)		Split torque, %	
			Due to backlash	Adjustment		
	Front-end spring rate, N/M (lb/in.)	Rear-end spring rate, N/M (lb/in.)	Face-down gear	Face-up gear	Face-down gear	Face-up gear
1	0 (Free float)	∞ (Restrained)	0.0 (0.0)	0.0 (0.0)	51.58	48.42
2	∞	↓	↓	↓	56.87	43.13
3	1.1×10^8 (6.0×10^5)[a]	1.1×10^8 = (6.0×10^5)[a]	↓	↓	53.11	46.89
4	1.1×10^7 (6.0×10^4)	↓	↓	↓	51.41	48.59
5	↓	↓	↓	0.0127 (0.0005)	51.55	48.45
6	↓	↓	↓	0.127 (0.005)	52.86	47.14
7	∞	↓	↓	↓	81.66	18.34
8	1.1×10^7 (6.0×10^4)	↓	0.076 (0.003)	0.0 (0.0)	50.54	49.46
9	↓	↓	0.127 (0.005)	↓	40.97	50.03

[a]1.1×10^8 N/M (6.0×10^5 lb/in.) is the translational spring rate for typical bearing and housing support in helicopter transmission.

The use of backlash control to compensate for the difference in the tangential stiffness between the two output shafts was investigated. In reality, the exact compliance between the teeth of the three gears is not practical. The deviation from the common engagement is caused not only by the different stiffness of the two paths but also by the indexing problem associated with the closed-loop gear train design. Additional analyses have been performed to incorporate the initial clearance on any one side of the pinion to simulate unequal backlash conditions. This was done by setting an initial clearance in the appropriate gap element. The influence of unequal backlash on load sharing in the split-torque drive system is also given in Table I. The effect of clearance on torque split was small but should be considered when fine-tuning a design for optimal load sharing. The analysis results are the baseline for using backlash control in assembling an equal torque-splitting drive in practice.

A structural dynamic analysis was carried out to determine a resonance free system by stiffening the fully compliant support at the front end of the pinion shaft. The selection of the pinion support with the designed spring rate to remain nearly equal torque splitting and to meet the structural dynamics criteria is the key to the design of the split torque mechanism. A few devices which may provide the compliance to obtain even torque splitting were studied. The torque split mechanism must be as compliant as possible yet stiff enough to ensure the frequency of the first vibrational mode is higher than the rotating speed of the pinion shaft to avoid resonance. The current effort in design concentrates on a squirrel cage spring support and a resilient bearing mount. The design should preclude any slip of the bearing outer ring. Also, the working range of the spring should be large enough for the movement of the pinion shaft to find its new center position of balance.

INFLUENCE OF GEAR ECCENTRICITY

The influence of gear eccentricity is important for determination of conditions of the split of torques when one pinion is in mesh with two face gears, and the pinion and the gears have eccentricity. Due to transmission errors the driven face gears will perform rotation with slightly different angular velocities, and this means that the split of torques will be accompanied with deflections of tooth surfaces.

Transmission error is defined as,

$$\Delta\phi_2' = \phi_2' - \frac{N_1}{N_2}\left(\phi_1' - \phi_1^*\right) \tag{1}$$

where N_1 and N_2 are the number of teeth of the pinion and the gear, respectively; ϕ_1' and ϕ_2' are the angles of rotation of the pinion and the gear, respectively; φ_1^* is the value of ϕ_1 that corresponds to $\phi_2' = 0$.

The results of investigation show that the transmission error curve due to eccentricity of the pinion or the gear only is an approximate harmonic curve. The periods of these curves are the time periods for one revolution of the pinion and the gear, respectively. The transmission errors for the case with eccentricity of both the pinion and the gear is a periodic function as shown in Fig. 4. The period of this curve is determined by the lowest common multiple of the numbers of teeth of the pinion and the gear.

The great advantage of face-gear drive with an involute pinion is that the pinion teeth are equidistant and have a common normal. This means at the end of the meshing of a pair of teeth and the beginning of meshing a next pair of neighboring teeth both tooth pairs will have a common normal. Therefore, the change of tooth meshing at the transfer point will not cause a jump of angular velocity.

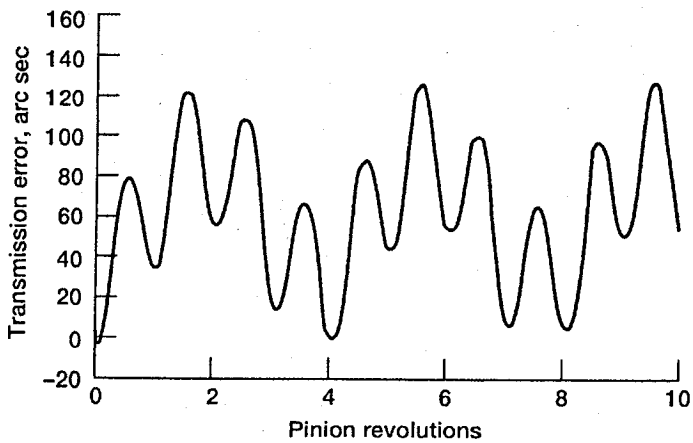

Figure 4.—Typical transmission errors for a face gear mesh.

This statement is correct as well for eccentric conventional involute gears. This implies that noise and vibration are relatively insensitive to gear misalignment.

BASIC TOPICS OF GEAR DESIGN AND MANUFACTURING

Generation of Face-Gear Drives with Localized Bearing Contact

The generation of the face gear by a shaper is shown in Fig. 5. The shaper and the gear rotate about intersecting axes with angular velocities $\omega^{(s)}$ and $\omega^{(2)}$ that are related as follows

$$\frac{\omega^{(s)}}{\omega^{(2)}} = \frac{N_2}{N_s} \qquad (2)$$

The designations of s and 2 indicate the shaper and the face gear, respectively.

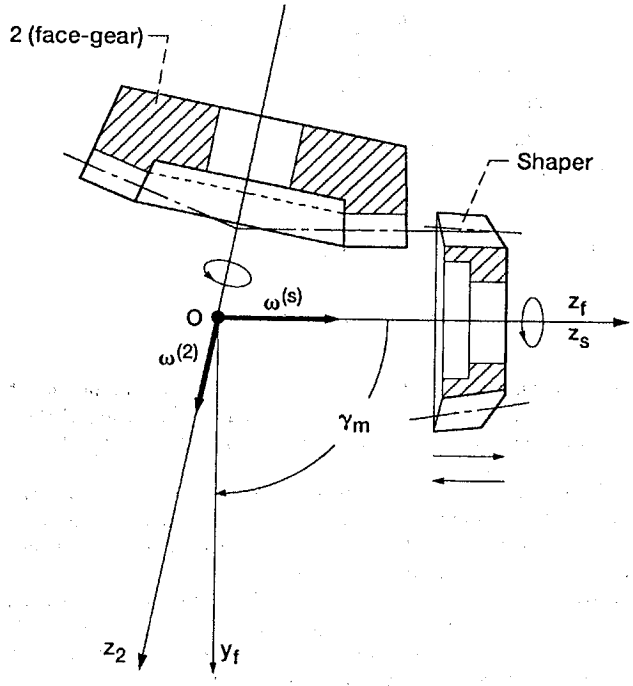

Figure 5.—Face-gear generation.

If the face gear is generated by a shaper that is identical to the pinion, the process of generation simulates the meshing of the pinion with the face gear being in *line* contact at every instant. In reality, such type of contact cannot be implemented due to its sensitivity to misalignment. The errors (tolerances) of assembly and manufacturing can cause separation of the contacting surfaces and results in the undesirable contact at the edge. To avoid this, it necessary to use a shaper with a larger number of teeth. The difference is denoted as $\Delta N = N_s - N_1$ (N_1 is the number of the pinion teeth; ΔN ranges from 1 to 3).

The geometric aspects of localization of bearing contact are illustrated with drawings of Fig. 6. We may imagine that three surfaces - Σ_s, Σ_1, and Σ_2 - are in mesh with each other simultaneously. Surfaces Σ_s and Σ_2 are in *line* contact at every instant in the process for generation. Surfaces Σ_s and Σ_1 are also in *line* contact being in an imaginary internal engagement as shown in Fig. 6. The imaginary meshing of the shaper and the pinion may be considered as a meshing with the following features: (1) the center distance B depends on the difference ΔN of the number of teeth of the shaper and the pinion; (2) there is an instantaneous axis of rotation that intersects the extended center distance O_sO_1 at point P and is parallel to the axes of the pinion and the shaper; (3) the instantaneous line of contact of Σ_s and Σ_1 is a straight line L_{s1} that is parallel to the axes of the shaper and the pinion; M is the point of intersection of L_{s1} with the plane of drawings; (4) surface Σ_s and Σ_2 are also in *line* contact (at L_{s2}) at every instant; and (5) surfaces Σ_2 and Σ_1 are in *point* contact and the instantaneous point of contact is the intersection of L_{s1} and L_{s2}.

The location of point P can be determined as the intersection of the common tangent to the base circles of the shaper and the pinion with the extended center distance O_sO_1 (Fig. 6). PM is the common normal to the involute shapes of the shaper and the pinion.

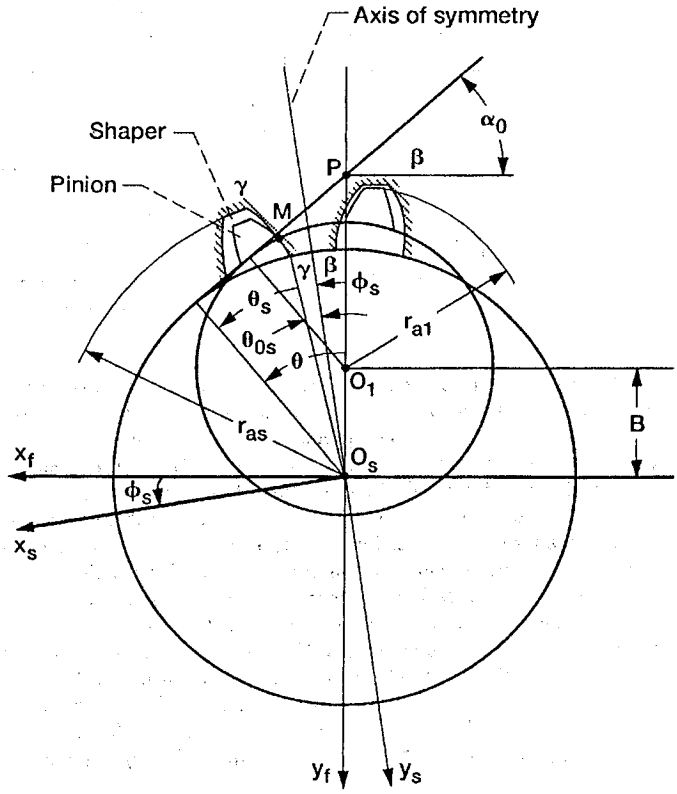

Figure 6.—Imaginary tangency of shaper and pinion surfaces.

The contact of the pinion and the face-gear surfaces under the load is a contact over an elliptical area; the center of such an ellipse is the theoretical contact point of Σ_2 and Σ_1.

The input design data for an example of a face-gear drive are given in Table II. These data are used for computations demonstrated in the following sections.

TABLE II. — INPUT FACE-GEAR DRIVE DESIGN DATA

Shaft angle, deg	80
Pinion number of teeth	28
Gear number of teeth	107
Diametral pitch	8
Pressure angle, deg	25

Meshing of the Shaper and the Face Gear

The shaper tooth surface Σ_s and the face-gear tooth surface Σ_2 contact each other at every instant at a spatial line L_{s2}. Contact lines on Σ_s and Σ_2 are shown in Fig. 7. The contact lines on Σ_s and Σ_2 are derived from the following equations (Litvin, 1989):

1. Contact lines on the shaper surface (Fig. 7 (a)) are defined as

$$\mathbf{r}_s(u_s,\theta_s), \quad N_s \cdot V_2^{(s2)} = f(u_s,\theta_s,\phi_s) = 0 \tag{3}$$

2. Contact lines on the face-gear surface (Fig. 7 (b)) are determined as

$$\mathbf{r}_2(u_s,\theta_s,\phi_s) = [M_{2s}(\phi_s)]\,\mathbf{r}_s(u_s,\theta_s), \quad f(u_s,\theta_s,\phi_s) = 0 \tag{4}$$

Here, (u_s,θ_s) are the Gaussian coordinates of the involute shaper surface (see Appendix A in Litvin et al., 1992) and ϕ_s is the generalized parameter of motion.

Tooth surface Σ_2 of the face gear is represented by Eqs. (4) in three-parametric form with an implicit relation between parameters (u_s,θ_s,ϕ_s). Fortunately, the equation of meshing

$$f(u_s,\theta_s,\phi_s) = 0 \tag{5}$$

is linear with respect to u_s and this enables us to eliminate u_s and represent Σ_2 in two-parametric form as

$$\mathbf{r}_2 = \mathbf{r}_2(\theta_s,\phi_s) \tag{6}$$

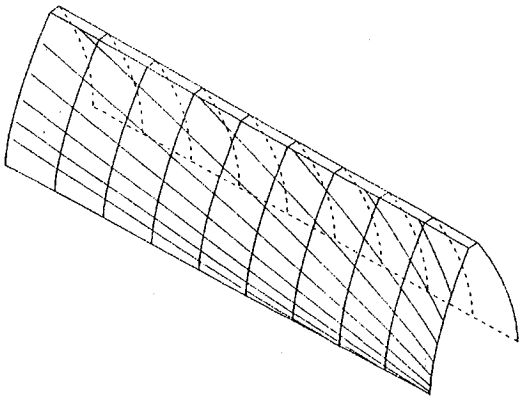

(a) Contact lines on shaper tooth surface.

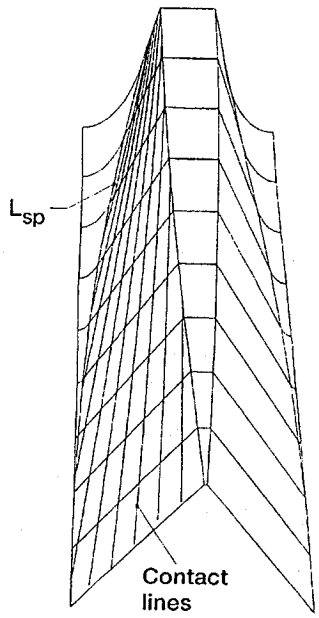

(b) Contact lines on face-gear surface.

Figure 7.—Face-gear contact lines.

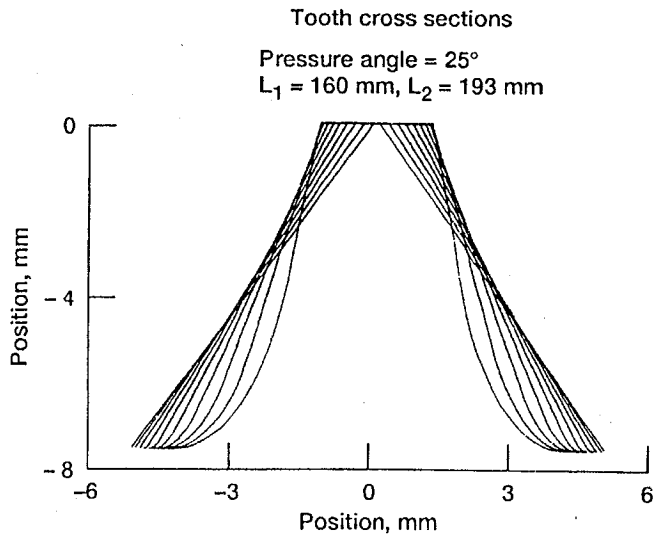

Figure 8.—Cross-sections of face-gear tooth surface.

Figure 8 shows the cross-sections of the face gear to depict the changing tooth profiles on Σ_2 and the pointing at the outside radius.

Limitations of Face-Gear Tooth Surface

The length of the tooth surface of a face gear is limited, due to the possibility of undercutting by the shaper in the dedendum area and the pointing of the teeth in the addendum area (Fig. 9).

The investigation of conditions of nonundercutting of the face gear is based on the theorem that has been proposed by Litvin (1989). There is a *limiting* line L on the generating surface (shaper surface Σ_s) that generates *singular* points on face-gear surface Σ_2. The limiting line on Σ_s can be determined with the equation

$$V_r^{(s)} + V^{(s2)} = 0 \tag{7}$$

Here; $V_r^{(s)}$ is the velocity of contact point in its motion *over* Σ_s; $V^{(s2)}$ is the sliding velocity of the shaper with respect to the face gear. The reflection line of the conjugate meshing part and the fillet on the face-gear tooth surface is designated by L_{sp} as shown in Fig. 7(b). More details are given in Appendix B in Litvin (1992).

The pointing of teeth (Fig. 7(b)) means that the tooth thickness on the top of the tooth becomes equal to zero. The location of the tooth pointing area may be determined by considering the intersection of the two opposite tooth surfaces at the top land of a tooth.

Computer programs for determination of limitations of the length of the face gears have been developed at the University of Illinois at Chicago. A quick review of results obtained are represented in the following charts.

Figure 9 shows the minimum and maximum radius factors for the face gear with various gear ratio m_{s2} and the shaper tooth numbers. In this example, the shaft angle is 80° and the pressure angle is 20°. The program is sufficiently general that it has the ability to generate design charts over a wide range. Knowing the values of minimum and maximum radius factor we can obtain the values of L_1 and L_2 (Fig. 10) by multiplying the radius factors by $N_2/2P$ where N_2 is the tooth number of the face gear and P is the diametral pitch. Using this method, L_1 and L_2 are in units of inches. For design convenience, a unitless design parameter $u_l = lP$ where $l = L_2 - L_1$ is usually considered. This parameter is similar to the parameter that express the ratio l/m where $m = 25.4/P$ is the module of spur or helical gears. For power transmissions it is desirable to keep $u_l \geq 7$. Our investigation shows that this can be obtained with the gear ratio (number of face

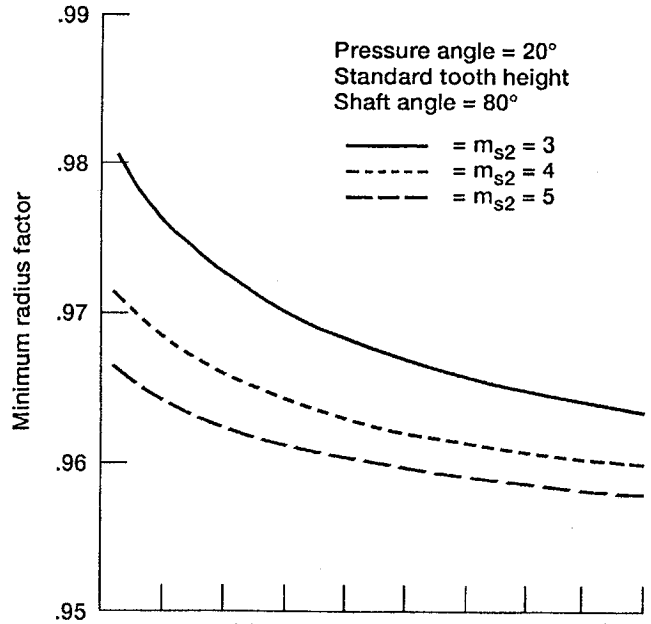

(a) Minimum radius factor.

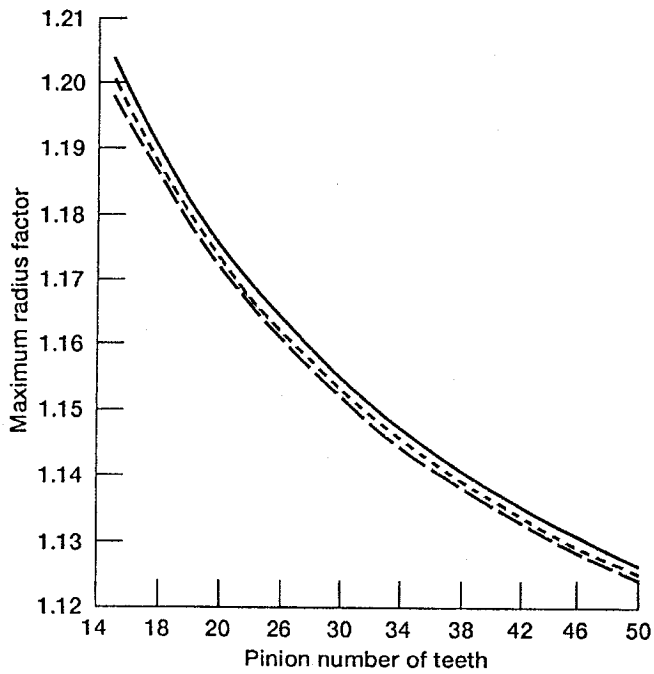

(b) Maximum radius factor.

Figure 9.—Face-gear minimum and maximum radius factors.

gear teeth divided by number of pinion teeth) ≥ 3.8. Using the data in Table II, we have obtained $L_1 = 160$ mm (6.3 in.), $L_2 = 193$ mm (7.6 in.).

Computerized Simulation of Meshing and Contact of Pinion and Face Gear

The bearing contact of pinion and face-gear tooth surfaces Σ_1 and Σ_2 is localized using the technique described in the previous section. Σ_1 and Σ_2 are in point contact at every instant. The computerized simulation of meshing and contact of Σ_1 and Σ_2 (Tooth Contact Analysis; TCA) can provide information on transmission errors and the shift of bearing contact that is caused by pinion-face-gear misalignment.

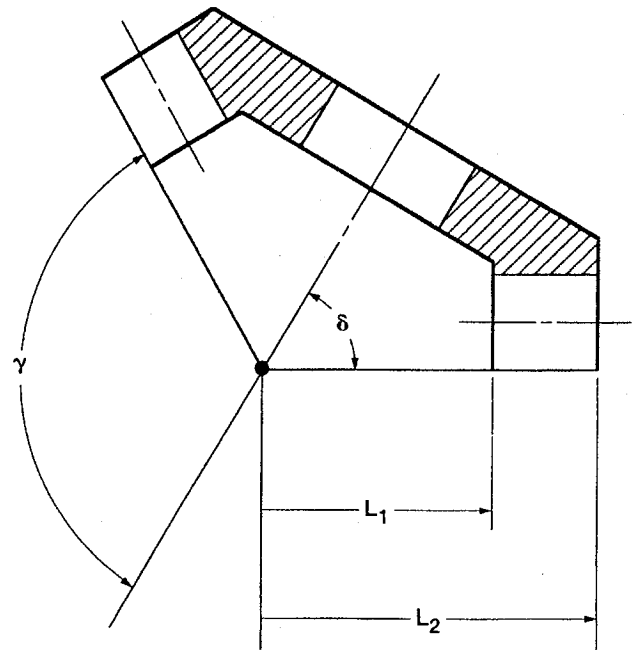

Figure 10.—The determination of face-gear tooth length.

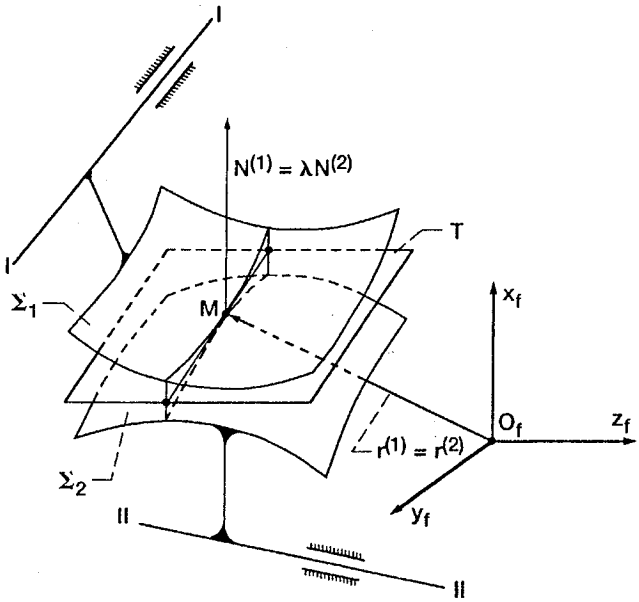

Figure 11.—Contact of mating surfaces.

The idea of TCA is based on equations of tangency of contacting surfaces (Fig. 11). Such equations express that the contacting surfaces Σ_1 and Σ_2 have, at any instant, a common position vector and collinear normals at their contact point M. For more details see Litvin (1989) (and Appendix C in Litvin, 1992).

Our investigation shows that the gear misalignment (change of the shaft angle, crossing of axes instead of intersection, axial displacement of face gear) does not cause transmission errors. This is a great advantage of face-gear drives in comparison with spiral bevel gear drive.

However, gear misalignment does result in the shift of the contact path on the gear surfaces. The patterns of the bearing contact can be determined considering the motion of the instantaneous contact ellipse over the pinion-gear tooth surfaces in the process of meshing. The dimensions and orientation of the instantaneous contact ellipse can be found if the prinicpal directions and

curvatures of the contacting surfaces are determined at the current point of surface contact (Litvin, 1992). The equations for computation of principal curvatures and directions are given in Appendix D in Litvin (1992). The elastic approach of the surfaces is considered as known.

It is possible to control the location of the bearing contact by changing of the machine angle γ_m that is formed by the axes of the shaper and the face gear. However, the small magnitude of $\Delta\gamma_m$ can be only implemented with a very precise control of γ_m. Figure 12 shows an example of the face-gear bearing contact prediction. The shift of bearing contact caused by gear misalignment and change in machine angle is given in Litvin (1992).

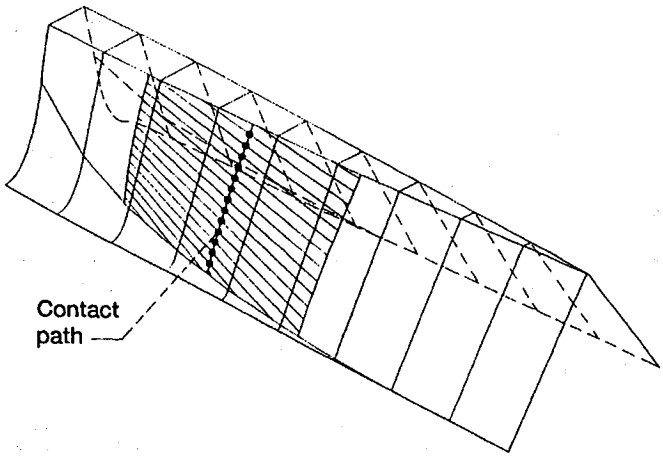

Figure 12.—Aligned face-gear drive: Localized bearing contact with $\Delta N = 3$.

Theoretical and Real Contact Ratio

The contact ratio m_c is determined with the equation

$$m_c = \frac{\phi_1^{(2)} - \phi_1^{(1)}}{\frac{360°}{N_1}} \tag{8}$$

Here; $\phi_1^{(2)}$ and $\phi_1^{(1)}$ represent the angles of rotation of the pinion that correspond to the beginning and the end of meshing for one pair of teeth; N_1 is the number of pinion teeth. Angles $\phi_1^{(2)}$ and $\phi_1^{(1)}$ can be determined from drawings of Fig. 7(b) that show the instantaneous contact lines referred to angles of pinion rotation. Taking into account that for drawings of Fig. 7(b) the stepsize of ϕ_1 is 3°, the number of contact lines that cover the surface of face gear is 10, and $N_1 = 28$ (see Table II), we obtain that the theoretical value of m_c is 2.33.

The localization of bearing contact is accompanied with the reduction of contact ratio, since the number of potential contact ellipses is reduced. Using an approach that is similar to the one discussed above, we have determined that $(\phi_1^{(2)} - \phi_1^{(1)})$ is 20.8°, and the real contact ratio is 1.62.

Generation of Face Gears by Rack-Cutter

The installment of the rack-cutter and the gear is as shown in Fig. 13. While the gear performs rotational motion about its axis, the rack-cutter performs translational motion in z_f axis.

The undercutting and pointing of the gear tooth surface limit the length of the generated face gears. For those design data listed in Table II, the tooth length P of the generated face gear is 0.3 in., which is too small for practical application (because $u_l = Pl = 2.4 < 7$).

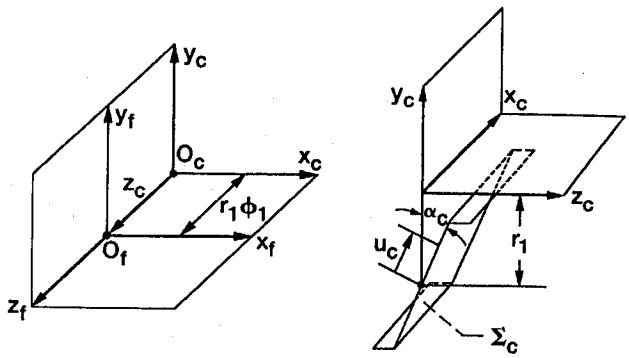

Figure 13.—Installment of the rack-cutter.

EXPERIMENTAL TESTS

Experimental tests on face gears were performed in the NASA Lewis spiral bevel gear rig (Handschuh et al., 1992). The face gears tested (Fig. 14) were basically a half-size version of the MDHC/Lucas ART design. The gears were 16 pitch with 28 teeth on the pinion and 107 on the face gear. The shaft angle was 90° to accommodate the rig. The gears were made of Maraging 300 steel per AMS 6514. The pinions were nitrided and ground with a case hardness of R_c 58. The face gears were shaper cut and hardened to R_c 52. For the tests, 100-percent design speed and torque were defined as 19 000 rpm pinion speed and 68 N/m (600 in./lb) pinion torque for a power of 135 kW (180 hp).

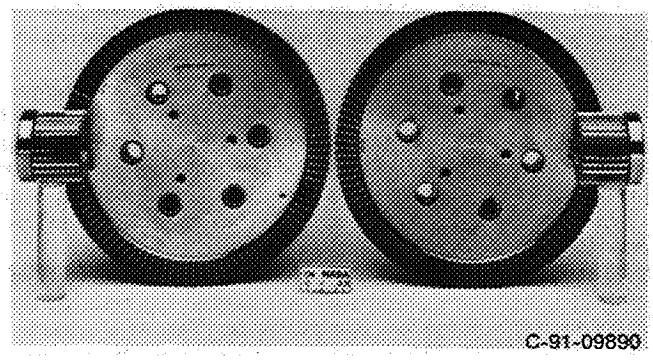

Figure 14.—Test gears.

The NASA Lewis spiral bevel gear rig (Fig. 15) operates on a closed loop or torque-regenerative principle. Two sets of pinion/face gears are used in the loop with the two pinions connected by a cross shaft. The outputs of the two face gears are connected through a helical gear mesh. A hydraulic loading system is connected to the helical mesh which puts a thrust load on the mesh, and thus, the torque in the loop. A variable speed motor is connected by a belt to the loop and powers the test stand.

A limited amount of test gears were available for test (four pinions and four face gears). The objective of the tests were to demonstrate the feasibility of face gears and determine the failure modes for high power applications. Four sets of gears successfully completed 26-hr (30×10^6 pinion cycles) endurance runs at 100-percent speed and torque. The gears were run at 74 °C (165 °F) oil inlet temperature using an ample supply of DOD-L-85734 lubricant at about 0.8 gpm per mesh. The contact pattern on the teeth was good and developed on the full tooth of the face gear. The pinion teeth showed normal wear. The face-gear teeth, however, had some surface distress. The teeth from the test side

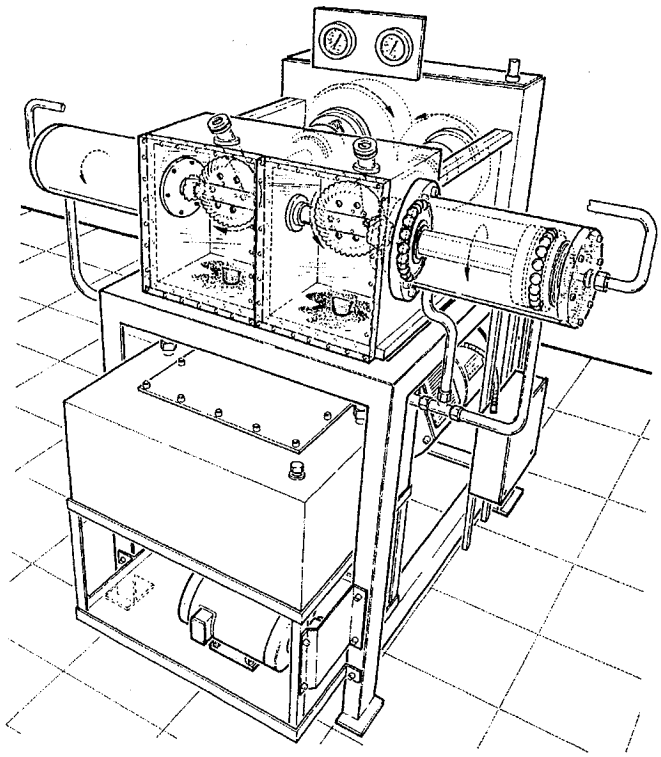

Figure 15.—NASA spiral bevel gear rig.

(pinion driving the face gear) had moderate wear and were in good condition. The teeth from the slave side (face gear driving the pinion) had small pit lines in some instances in the middle region of the teeth.

The gears were subsequently run 26 hr at 200-percent torque and 100-percent speed. One test (two sets of gears) lasted the 26 hr with the pinions showing moderate wear and the face gears showing increasing surface distress. The second test (the additional two sets of gears) was suspended after about 10.5 hr due to a tooth breakage on one of the face gears (slave side). The breakage originated from the surface pit line from the previous test.

The results, although limited, demonstrated the feasibility of face gears in high-speed, high-load applications. The tests did show surface distress with the face gears, however. The use of a hardened, ground gear steel (in use for conventional aircraft gears today but not presently available for face gears since manufacturing techniques do not exist to grind face gear) would significantly increase the surface durability and make face gears available for high-power application.

CONCLUSIONS

The use of face gears in helicopter transmissions was explored. A light-weight, split torque transmission design utilizing face gears was described. Face-gear design and geometry were investigated. Topics included tooth generation, minimum inner and maximum outer radii, tooth contact analysis, contact ratio, gear eccentricity, and structural stiffness. Face-gear experimental studies were also included. The following results were obtained:

1. The feasibility of face gears in high-speed, high-load applications such as helicopter transmissions was demonstrated through experimental testing. Face gears which were basically a half-scale version of the MDHC/Lucas ART design were tested in the NASA Lewis spiral bevel rig. The pinions and the gears showed good contact patterns and ran at 100- and 200-percent design torque. However, the face gears did have some surface distress.
2. Analytical transmission error studies showed face-gears were relatively insensitive to gear misalignment. Tooth contact, however, was affected by misalignment resulting in a shift of the contact on the tooth surfaces. A method of localizing contact by changing tool settings of the generating machine was explored.
3. The length of the face-gear tooth width was limited due to possible undercutting by the shaper in the dedendum area and pointing of the teeth in the addendum area. Design charts were developed to determine minimum inner and maximum outer radii.
4. A finite element analysis of the pinion and face-gear structure in a split torque design provided data on load sharing. Among the cases studied, an even torque split was provided when the stiffness of the pinion shaft front support (close to the face-gear mesh) was about an order of magnitude less than a typical bearing support.

ACKNOWLEDGMENT

The authors express their gratitude to Mr. Luis Bohorquez and Mr. R.J. King (McDonnell Douglas Helicopter Company) and Mr. Robert Handschuh (U.S. Army Propulsion Directorate, NASA Lewis) for their invaluable support of this research project.

REFERENCES

Bill, R.C., 1990, Advanced Rotorcraft Transmission Program, NASA TM-103276.

Bossler, R.B., and Heath, G.F., 1990, Advanced Rotorcraft Transmission (ART Program Status, presented at the American Helicopter Society Rotary Wing Propulsion Specialists Meeting, Williamsburg, VA, Nov. 13-15, preprint No. 2.

Bossler, R.B., and Heath, G.F., 1991, Advanced Rotorcraft Transmission (ART) Program Status, presented at the Joint Propulsion Conference, June 24-27, Sacramento, CA.

Buckingham, E., 1949, Analytical Mechanics of Gears, Dover Publications, N.Y.

Dudley, D.W., 1962, Gear Handbook, McGraw-Hill Book Company.

Davidov, J.S., 1950, Noninvolute Gearing (in Russian), Mashgiz.

Litvin, F.L., 1968, Theory of Gearing (in Russian), 2nd edition, Nauka.

Litvin, F.L., 1989, Theory of Gearing, NASA RP1212.

Litvin, F.L., et al., 1992, Design and Geometry of Face-Gear Drives, accepted for publication in *Journal of Mechanical Design*.

Handschuh, R.F., Lewicki, D.G., and Bossler, R., 1992, Experimental Testing of Prototype Face Gears for Helicopter Transmissions, NASA TM-105434, USAAVSCOM 7R-92-C-008.

REPORT DOCUMENTATION PAGE

Form Approved
OMB No. 0704-0188

1. AGENCY USE ONLY (*Leave blank*)	2. REPORT DATE	3. REPORT TYPE AND DATES COVERED
	1992	Technical Memorandum

4. TITLE AND SUBTITLE

Application of Face-Gear Drives in Helicopter Transmissions

5. FUNDING NUMBERS

WU–505–63–36
1L162211A47A

6. AUTHOR(S)

F.L. Litvin, J.-C. Wang, R.B. Bossler, Jr., Y.-J.D. Chen,
G. Heath, and D.G. Lewicki

7. PERFORMING ORGANIZATION NAME(S) AND ADDRESS(ES)

NASA Lewis Research Center
Cleveland, Ohio 44135–3191
and
Propulsion Directorate
U.S. Army Aviation Systems Command
Cleveland, Ohio 44135–3191

8. PERFORMING ORGANIZATION REPORT NUMBER

E–7019

9. SPONSORING/MONITORING AGENCY NAMES(S) AND ADDRESS(ES)

National Acronautics and Space Administration
Washington, D.C. 20546–0001
and
U.S. Army Aviation Systems Command
St. Louis, Mo. 63120–1798

10. SPONSORING/MONITORING AGENCY REPORT NUMBER

NASA TM–105655
AVSCOM TR–91–C–036

11. SUPPLEMENTARY NOTES

Prepared for the Sixth International Power Transmission and Gearing Conference sponsored by the American Society of Mechanical Engineers, Scottsdale, Arizona, September 13–16, 1992. F.L. Litvin and J.-C. Wang, University of Illinois at Chicago, Chicago, Illinois 60680. R.B. Bossler, Jr., Lucas Western, Incorporated, City of Industry, California 91749. Y.-J.D. Chen and G. Heath, McDonnell Douglas Helicopter Company, Mesa, Arizona 85205. D.G. Lewicki, Propulsion Directorate, U.S. Army Aviation Systems Command. Responsible person, D.G. Lewicki, (216) 433–3970.

12a. DISTRIBUTION/AVAILABILITY STATEMENT

Unclassified - Unlimited
Subject Category 37

12b. DISTRIBUTION CODE

13. ABSTRACT (*Maximum 200 words*)

The use of face gears in helicopter transmissions was explored. A light-weight, split torque transmission design utilizing face gears was described. Face-gear design and geometry were investigated. Topics included tooth generation, limiting inner and outer radii, tooth contact analysis, contact ratio, gear eccentricity, and structural stiffness. Design charts were developed to determine minimum and maximum face-gear inner and outer radii. Analytical study of transmission error showed face-gear drives were relatively insensitive to gear misalignment, but tooth contact was affected by misalignment. A method of localizing bearing contact to compensate for misalignment was explored. The proper choice of shaft support stiffness enabled good load sharing in the split torque transmission design. Face-gear experimental studies were also included and the feasibility of face gears in high-speed, high-load applications such as helicopter transmissions was demonstrated.

14. SUBJECT TERMS

Transmission (machine elements); Gears; Design; Helicopters

15. NUMBER OF PAGES

10

16. PRICE CODE

A02

17. SECURITY CLASSIFICATION OF REPORT	18. SECURITY CLASSIFICATION OF THIS PAGE	19. SECURITY CLASSIFICATION OF ABSTRACT	20. LIMITATION OF ABSTRACT
Unclassified	Unclassified	Unclassified	